

Low-order Wavefront Error Compensation for Multi-field of Lithography Projection Objective Based on Interior Point Method

LU Yutong, ZHOU Ji, KANG Xia, ZHU Xianchang, LIU Junbo, WANG Jian, HU Song

(Institute of Optics and Electronics, Chinese Academy of Sciences, Chengdu, China 610209)

Abstract: Low-order wavefront error account for a large proportion of wave aberrations. A compensation method for low order aberration of projection lithography objective based on Interior Point Method is presented. Compensation model between wavefront error and degree of movable lens freedom is established. Converting over-determined system to underdetermined system, the compensation is solved by Interior Point Method (IPM). The presented method is compared with direct solve the over-determined system. Then, other algorithm GA, EA and PS is compared with IPM. Simulation and experimental results show that the presented compensation method can obtained compensation with less residuals compared with direct solve the over-determined system. Also, the presented compensation method can reduce computation time and obtain results with less residuals compare with AGA, EA and PS. Moreover, after compensation, RMS of wavefront error of the experimental lithography projection objective decrease from 56.05 nm to 17.88 nm.

Keywords: Wavefront Error Compensation, Lithography Projection Objective, Interior Point Method, Computer Aided Alignment

1 Introduction

The phase deviation of each point on the exit pupil of an optical system relative to the ideal wavefront is called the wave aberration of the system^[1]. Compared with image quality evaluation methods such as resolution and point spread function, it can characterize the imaging quality of the optical system more effectively and directly. At present, the analysis and compensation of wave aberration in projection lithography objective systems are mostly based on the Fringe Zernike polynomial fitting of the pupil function - the root mean square value of wave aberration. The Fringe Zernike intuitively divides the aberration by a polynomial in a symmetrical relationship with the angle^[2]. According to the fitting

result of the Fringe Zernike polynomial for wave aberration, the wave aberration of the optical system can be divided into low-order aberrations of Z1-Z9 terms, and high-order aberrations from Z10 terms to higher-order terms. The Z1-Z4 items correspond to 00-10 aberrations, which can be compensated by adjusting the image plane^[3].

In early period, the image quality compensation of optical systems only adjusted the position of components according to the collected interferogram. This method is highly depended on the operator's experience, and the adjustment efficiency and effect are limited^[4].

David M. Williamson and others of Perkin-Elmer Company compensated the system aberration from

98nm to 18nm by adjusting the component position parameters for the aberration compensation of the i-line objective^[5].

In 2003, Nikon developed a projection objective with a wavelength of 193 nm and a numerical aperture of 0.78. Through stricter error control, the system wave aberration is converged from 40nm to 2nm^[6].

With the advent of immersion projection lithography objectives, a series of more complex compensation methods have emerged. The wave aberration of ASML's 1900i lithography machine and Nikon's S620D lithography machine can finally be controlled below 1nm^[7-8].

In summary, at present the image quality compensation measures used in the integration and use of lithography objective lenses mainly include: computer-aided adjustment technology^[9], optical complex calculation and component surface shape refinement technology. In addition, it also includes some dynamic compensation technologies, such as real-time deformable mirror adjustment technology and infrared thermal compensation technology^[10-11].

Since the image quality compensation of the projection lithography objective is a process throughout the entire service cycle of the system, the operability and adjustment efficiency of the compensation measures for the projection objective are very important. In order to realize the aberration compensation of the whole life cycle of the objective optical system, it is necessary to establish a corresponding mathematical model. Some of the actual regulatory constraints are involved in existing common compensation model such as actuator stroke. Also to satisfy all the constraints, multiple calculations are needed, which may takes a lot time. This will reduce work efficiency during machine operating.

In this paper, based on the Fringe Zernike coefficient of wave aberration, a low-order wavefront error compensation for multi-field of lithography projection objective based on IPM (Interior Point Method) are proposed. Converting over-determined system to underdetermined system, better optimization results and computational speed are

obtained. IPM (Interior Point Method) are used to solve the compensation. Simulation and experimental work are carried out to verify the method. This method has a good compensation effect for the low-order aberrations of Z4-Z9 terms which account for a large proportion in the lithography projection objective lens, and realize the image quality compensation optimization of the high NA lithography projection objective lens.

2 Wavefront Error Compensation Model

The difference between the design value and the actual value of the lithography projection objective optical system will bring system aberration. The relationship between the image quality of the optical system and the position parameters of the component structure can be expressed by the Eq.(1)^[12].

$$\begin{bmatrix} F_1 \\ \vdots \\ F_m \end{bmatrix} = \begin{bmatrix} f_1(z_1 \cdots z_n) \\ \vdots \\ f_m(z_1 \cdots z_n) \end{bmatrix} \quad (1)$$

In the formula, F_j ($j=1, 2, \dots, m$) represents the image quality of the optical system; z_i ($i=1, 2, \dots, n$) represents the structural parameters of each component; f_j ($j=1, 2, \dots, m$) represents the functional relationship between image quality and structural parameters.

When using moving mirror for image quality compensation, the complex function relation between aberration and structural parameters can be simplified to linear relation due to the adjusted structural parameters vary in a small range. Therefore, the relationship between the aberration and the structural parameters of the system in the process of image quality compensation can be expressed as linear Eq.(2)^[8]

$$\begin{bmatrix} F_1 \\ \vdots \\ F_m \end{bmatrix} = \begin{bmatrix} F_{01} \\ \vdots \\ F_{0m} \end{bmatrix} + \begin{bmatrix} \frac{\partial f_1}{\partial z_1} \Delta z_1 + \cdots + \frac{\partial f_1}{\partial z_n} \Delta z_n \\ \vdots \\ \frac{\partial f_m}{\partial z_1} \Delta z_1 + \cdots + \frac{\partial f_m}{\partial z_n} \Delta z_n \end{bmatrix} \quad (2)$$

The equations are expressed in the matrix form as Eq.(3):

$$\mathbf{S}^* \mathbf{Z} = \mathbf{X} \quad (3)$$

$$\text{where, } \mathbf{S} = \begin{bmatrix} \frac{\partial f_1}{\partial z_1} & \dots & \frac{\partial f_1}{\partial z_n} \\ \vdots & \ddots & \vdots \\ \frac{\partial f_m}{\partial z_1} & \dots & \frac{\partial f_m}{\partial z_n} \end{bmatrix}, \quad \mathbf{Z} = \begin{bmatrix} \Delta z_1 \\ \vdots \\ \Delta z_n \end{bmatrix},$$

$$\mathbf{X} = \begin{bmatrix} F_1 \\ \vdots \\ F_m \end{bmatrix} - \begin{bmatrix} F_{01} \\ \vdots \\ F_{0m} \end{bmatrix}$$

\mathbf{S} is the tolerance sensitivity of the optical system, which is only related to the system structure itself and can be solved by the optical design software. \mathbf{X} is the change of optical system structural parameters. \mathbf{Z} is the difference between the actual value and the ideal value of the image quality of the optical system.

\mathbf{S} and \mathbf{Z} are known quantity in image compensation solution. The adjustment of the corresponding compensation parameter can be obtained by solving for \mathbf{X} .

For the lithography projection objective optical system in this paper, 5 sampling points are selected from the square field of view of 10mm×10mm for image quality evaluation and calculation. The sensitivity matrix is a matrix of m rows and n columns. m is the number of all image quality evaluation parameters, and n is the number of compensators. As is shown in the Eq.(4), is the concrete matrix form of \mathbf{S} .

$$\mathbf{S} = \begin{bmatrix} \text{Field}_{11} \begin{Bmatrix} Z_5 \\ \vdots \\ Z_9 \end{Bmatrix} & \dots & \text{Field}_{n1} \begin{Bmatrix} Z_5 \\ \vdots \\ Z_9 \end{Bmatrix} \\ \vdots & \ddots & \vdots \\ \text{Field}_{1m} \begin{Bmatrix} Z_5 \\ \vdots \\ Z_9 \end{Bmatrix} & \dots & \text{Field}_{nm} \begin{Bmatrix} Z_5 \\ \vdots \\ Z_9 \end{Bmatrix} \end{bmatrix} \quad (4)$$

The compensation model (Eq.(3)) is a overdetermined equation system. The compensation could be obtained by solving the overdetermined system. There are only the least squares solution for the compensation model. However in general, the least squares solution does not meet the actual constraints, such as the actuator stroke limit. Therefore, it is necessary to solve a set of compensation \mathbf{X} satisfying the actuator stroke to make the residual within the allowable tolerance. This problem is converted to

finding a compensation result \mathbf{Z} in the tolerance so that the equation system has a certain solution.

The conditions for the equation system having certain solutions are as follows:

$$r(\mathbf{S}) = r(\bar{\mathbf{S}}) \leq N \quad (5)$$

in which, N is the degree of freedom, $\bar{\mathbf{S}}$ is the augmented matrix of \mathbf{S} , $\bar{\mathbf{S}} = [\mathbf{S}|\mathbf{Z}]$, $r(\cdot)$ is the rank of matrix.

The singular value of Sensitivity Matrix \mathbf{S} and the augmented matrix $\bar{\mathbf{S}}$ are obtained by SVD Decomposition, which are $[\sigma_1 \sigma_2 \dots \sigma_r]$ respectively. Then, the condition Eq.(6). can be meet when each item of $[\sigma_{r+1} \dots \sigma_p]$ is 0. Each item of $[\sigma_{r+1} \dots \sigma_p]$ is linearly related. By extracting coefficients, the following equation system can be obtained:

$$\mathbf{A} * \mathbf{Z} = \mathbf{b} \quad (6)$$

Equation system Eq.(6) is a underdetermined system for $r(\mathbf{A}) < N_z$, where N_z is the number of item for \mathbf{Z} . equation system Eq.(6) is solved by optimization algorithm. The optimization objectives are:

Satisfaction degree of Eq.(6)

$$fit1 = \sqrt{\|\mathbf{A} * \mathbf{Z} - \mathbf{b}\|} \quad (7)$$

The contribution value to RMS after compensation

$$fit2 = \sqrt{\|\mathbf{Coeff} * \mathbf{Z}\|} \quad (8)$$

where, $\|\cdot\|$ is the inner product operator, \mathbf{Coeff} is proportion of $Z_5 \sim Z_9$ in RMS.

Euler distance of Eq.(7) and Eq.(8) are taking as the optimization objective to convert the multi-objective optimization to a single objective optimization:

$$\min(fit), \quad fit = \sqrt{fit1^2 + fit2^2} \quad (9)$$

The value of \mathbf{Z} is within the allowable range of compensation residuals.

Constraint condition of the optimization is:

$$\mathbf{X} = \mathbf{Z} * \mathbf{S}^H \in \Omega \quad (10)$$

Where, \mathbf{S}^H is the generalized inverse of sensitivity matrix, Ω is the region satisfying actuator stroke.

3 Numerical Calculation by Interior Point Method

Interior Point Method (IPM) is used to solve the constrained optimization. IPM starts from the interior point in the iteration and keeps searching within the feasible region. And the constrained optimization is transformed into unconstrained by introducing barrier function. Then, this unconstrained optimization are solved iteratively by New-ton method. Also, the barrier function is updated continuously during optimization it-erative process to make the algorithm converge. Pseudocode of the algorithm is shown in Table 1.

After adding a barrier function to the original optimization objective Eq.(11), the new optimization objective becomes:

The barrier function is as follows:

$$\min(\text{fit}(\mathbf{Z}) + B(\mathbf{Z})) \quad (11)$$

Logarithmic function is used as barrier function $B(X)$. when approaching boundary condition, the objective function value will sharply increase cause of barrier function $B(Z)$.

$$B(\mathbf{Z}) = -\frac{1}{t} \log(-(\mathbf{Z} * \mathbf{S}^H - X_{lim})) \quad (12)$$

where, t is a coefficient and X_{lim} is the max actuator stroke, in following simulation, $t=1$.

Table 1 Interior Point Method for Multi-field Aberration Compensation

Algorithm: Interior point method for multi-field aberration compensation

Input: Target compensation result Z^0 compensation result tolerance Tol Sensitivity matrix S max actuator stroke X_{lim} convergence criteria $tol1$, $tol2$ maximum iteration step max_i

- 1 Calculating singular values of augmented trix $[S|Z]$
- 2 Extract coefficient matrix A 、 b according to solution condition of equation
- 3 For $i=1: max_i$
- 4 $fun^i = \text{fit}(Z^i) + B(Z^i)$
- 5 $Z^{i+1} = Z^i - fun^i / \nabla fun^i$
- 6 if $\frac{Z^{i+1} - Z^i}{Z^{i+1}} < tol1$ or $fun^i < tol2$, then
- 7 $Z = Z^i$
- 8 break
- 9 end
- 10 end
- 11 $X = Z * S^H$

Output: Compensation X

4 Simulation

4.1 Performance Index Test of the Solar Simulator

The structure of the lithography projection objective optical system used in this paper and the compensator settings are shown in the Fig.1. The sampling points used for image quality compensation are marked in red. The system consists of 23 full transmission lens, and the central wavelength (λ) is 365nm. The square field of view, as shown in Fig.2, is 10mm×10mm. Five field-of-view points are selected for the calculating of the wavefront error compensation of the li-thography projection objective optical system.

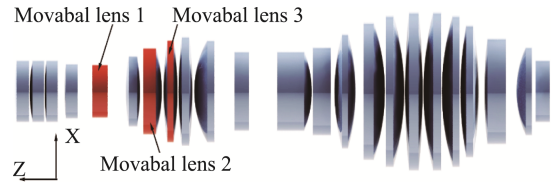


Fig.1 Optical System Structure & Compensator Position

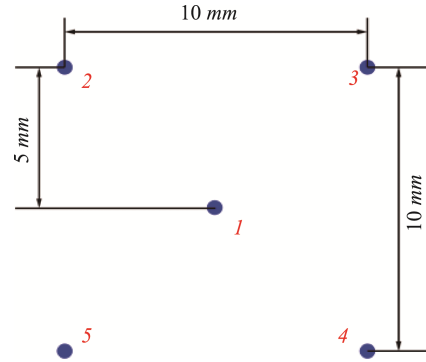


Fig.2 Field Position

4.2 Sensitivity Matrix

In order to ensure that the lithography projection objective lens can be as close to the design value as possible after integrated installation and adjustment, component tolerances need to be properly allocated. Combined with the system structure and the existing processing level, the system tolerances are set as follows:

Using the optical design software for simulation, the initial values of the image quality pa-rameters of the projection optical system to be compensated are obtained as shown in the Table 3.

Table 2 Tolerance Settings for Projection Objectives

Tolerance Type	DLR/mm	DLT/mm	DSZ/mm	TIL/''	DIS/mm	DLN/ppm
Tolerance Limits	0.001	0.001	0.001	1	0.005	10

Table 3 Image Quality Parameters of Tolerated Objectives

Coefficient	Z5/ λ	Z6/ λ	Z7/ λ	Z8/ λ	Z9/ λ	RMS Wavefront Error/ λ
F1	-2.21E-12	0.00E+00	0.00E+00	0.00E+00	4.33E-04	0.006
F2	-2.75E-11	-0.00119	-0.00699	0.006992	-1.28E-03	0.0087
F3	1.12E-11	0.001192	0.006992	0.006992	-1.28E-03	0.0087
F4	-2.64E-11	-0.00119	0.006992	-0.00699	-1.28E-03	0.0087
F5	-2.75E-11	0.001192	-0.00699	-0.00699	-1.28E-03	0.0087

The wavefront error variation with lens moving along a certain degree of freedom are calculated. The lens movement along the optical axis is -10~10um. And the lens rotation around sagittal and meridian direction are all -10~10 second. The item variation with the worst linearity in Zernike sub-items at each field during lens moving are shown in Fig.3. As the lens moves and rotates, each share of Zernike changes linearly with linearly dependent coefficient below 0.3. Then, the simulation result is fitted with linear function, and the slope of which is the sensitivity coefficient. Sensitivity is consist of the sensitivity coefficient between different Zernike terms and degrees of freedom at each field.

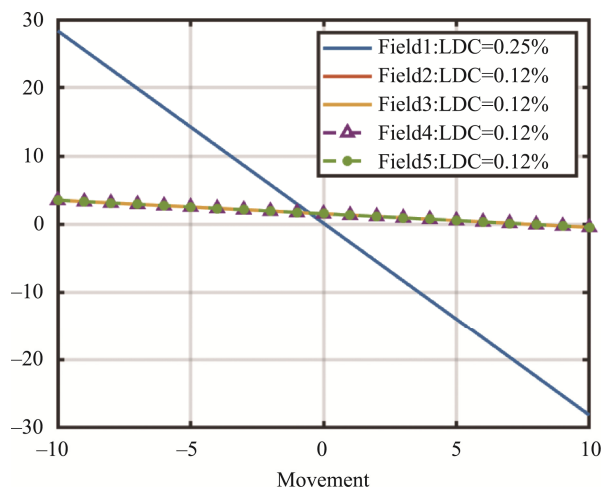


Fig.3 Wavefront Error Variation with Lens Moving /nm

4.3 Simulation Analysis

A set of wavefront error is simulated considering manufacture, assembly, tem-perature, pressure and material effect by monte carlo simulation. And the wavefront error is compensated with the sensitivity matrix in 4.2. The compensation X is calcu-lated by IPM (Interior Point Method) and AGA (Adaptive Genetic Algorithm) respec-tively. Also, multi-objective optimization are also calculated to verify the effect con-verting into single-objective optimization. Throught the multi-objective optimization, Pareto optimal solution is obtained. EA (Evolution Algorithm) and PS (Pattern Search) are used to solve the multi-objective optimization. Computing environment are Intel I7-11800H 16G /RTX3060.

Iteration of compensation calculation by Single objective optimization interior point method and AGA (Adaptive Genetic Algorithm), and multi-objective optimiza-tion by EA (Evolution Algorithm) and Pattern search are shown in Fig.4. By IPM, the best optimization result are obtained among the four calculation method, with fit=79.259. fit by IPM is lower with 19.32%, 18.58%, and 14.34% by AGA, EA, and PS respectively.

The computing time of each algorithm is shown in Fig.5 IPM performs best among the four algorithm in computing time with 1.12s.

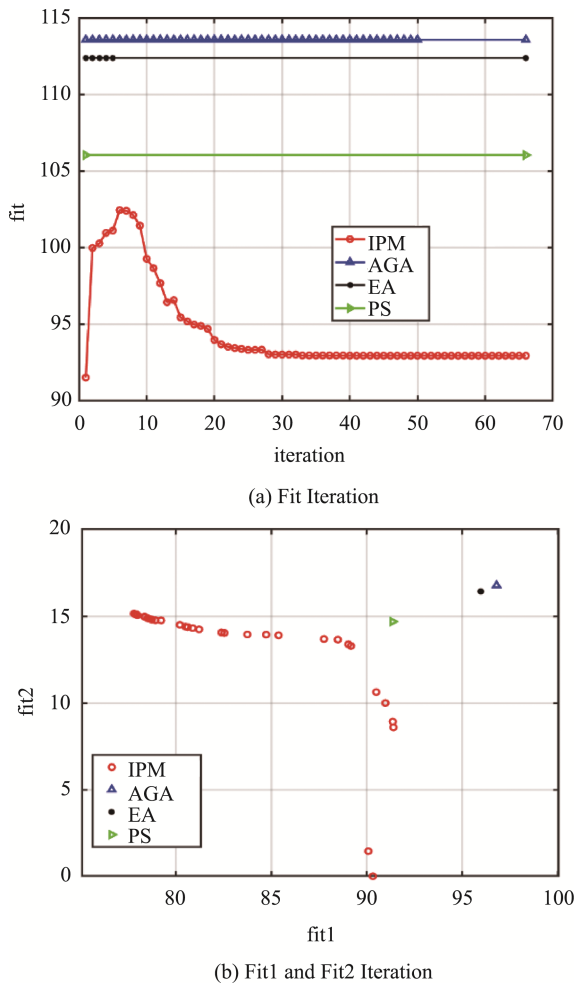


Fig.4 Compensation Calculation Iteration

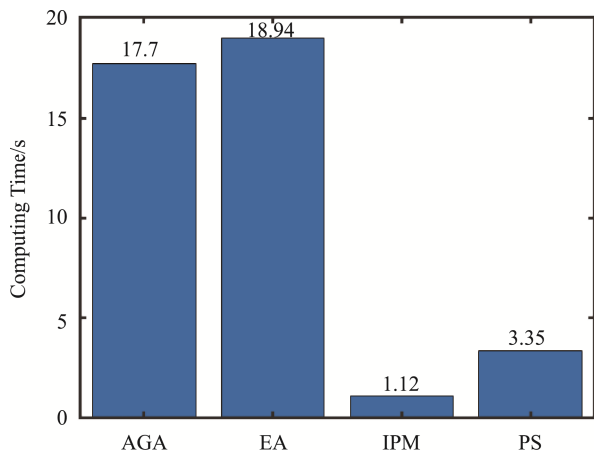


Fig.5 Computing Time

Compensation residual error for each algorithm is shown in Fig.6. The four optimization algorithm

perform differently at each field. The final convergence result is a balance for each field.

Compare the direct optimization solution Eq.(3) between the proposed reversal method, the compensation residual error are shown in Fig.7. The compensation residual error is decreased by 39.32% in maximum. The proposed reversal method can obtain better optimization results.

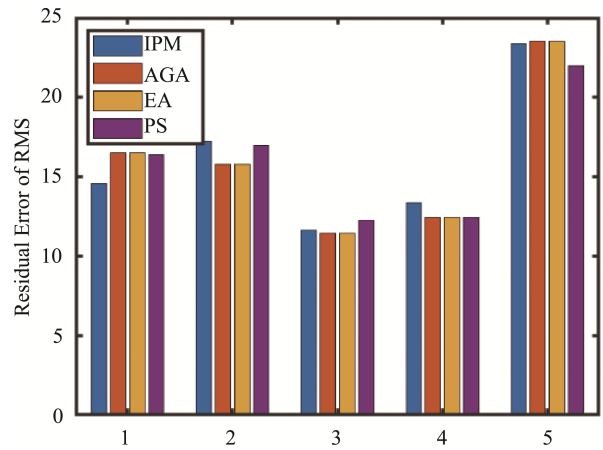


Fig.6 Residuals after Compensation by Different Algorithm

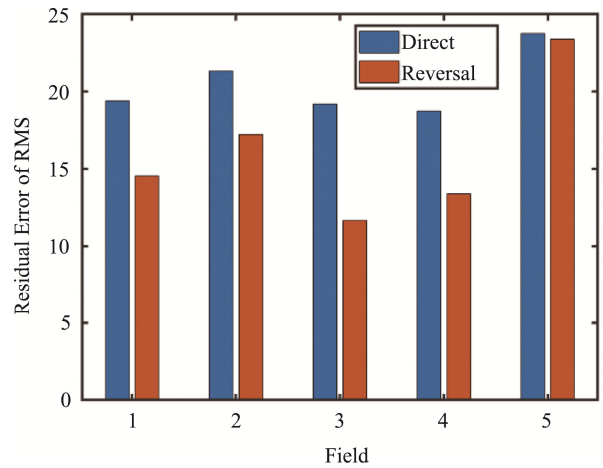


Fig.7 Residuals after Compensation by Different Model

5 Experimental Work

Experiment is designed to verify the compensation effect. The experimental system is shown in Fig.8. The

parameter of lithography projection objective is the same as 4.1. And the wavefront error is tested by Shack-Hartmann wavefront sensor. The Shack-Hartmann wavefront sensor assembled at the bottom aberration test system. A scanner mounted in the top to scanning each field. And the field position is the same as Fig.2.

The sensitivity matrix is calibrated in the first. The lens moves along nine degrees of freedom between 0~50 um by 10um step.25 samplings at per movement and the mean value are taken. The sensitivity matrix is the slope of fitting line.

Initial wavefront error each field of the lithography projection objective is shown in Fig.9 and Fig.10. The maximum RMS is 56.05 nm. After compensation by IPM, the result is shown in Fig.9 and Fig.10. The maximum RMS is 17.88 nm. Compared with initial state, RMS of wavefront error decrease by 68.1%.

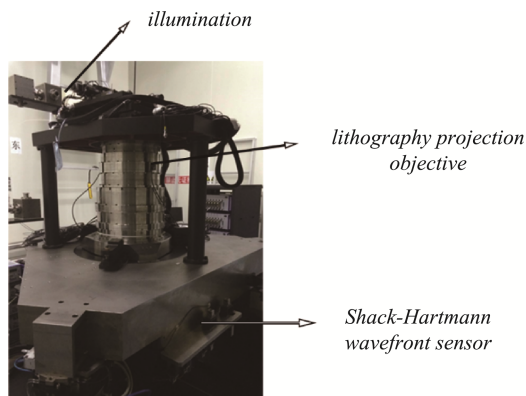


Fig.8 Experimental System

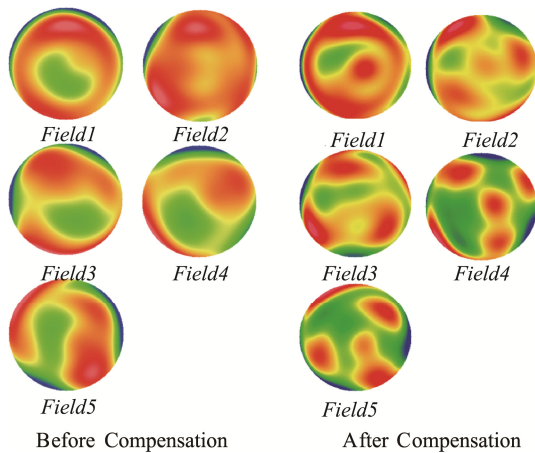


Fig.9 Wavefront before and after Compensation

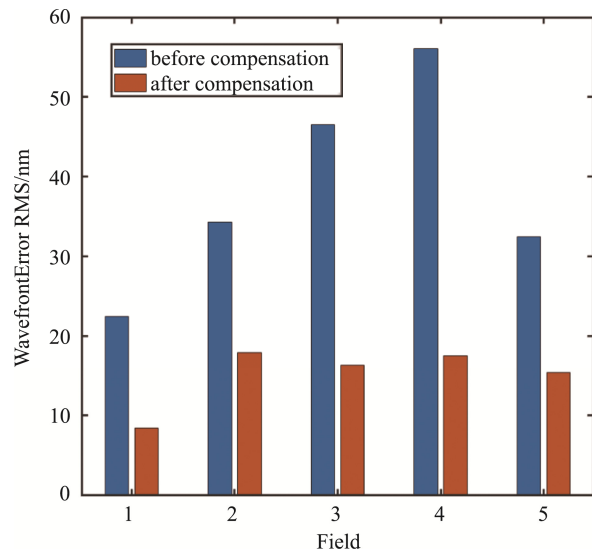


Fig.10 Wavefront Error (RMS) before and after Compensation

6 Conclusion

In this paper, a lower-order wavefront error compensation for multi-field of lithography projection objective based on IPM (Interior Point Method) are proposed. Converting overdetermined system to underdetermined system, better optimization results and computational speed are obtained. IPM (Interior Point Method) are used to solve the compensation. Simulation and experimental work are carried out to verify the method. Conclusions are as follows:

1. The compensation calculation method can compensate the low-order wavefront aberration, compared with initial state, RMS of wavefront error decrease by 68.1 % in the test.
2. The compensation calculation method proposed in this paper performs well at low-order wavefront error compensate. Experimental results show that after compensation by IPM, the RMS reduced to 17.88 nm, and decrease by 68.1% compared with initial state.
3. The compensation calculation method proposed in this paper can obtain better results with less residuals compare with AGA, EA and PS. And minimum computation time by IPM is consumed efficient with 1.12s.
4. Converting over-determined system to under-determined system, difficulty in optimization is

reduced so that the algorithm can converge to better compensation. Compare with the direct optimization solution, the compensation residual error is decreased by 39.32% in maximum.

References

- [1] LINQ, JINCH SH, XIANGP, et al. "Computer-aided alignment of Schwarzschild objective with off-axis illumination," *J. Opt. Precision Eng*, 11(2): 144–150, (2003).
- [2] Xu Weicai. "Optical Design and Imaging Performance Compensation for the Lithographic Lens," D. Changchun: Changchun Institute of Optics, Fine Mechanics and Physics, Chinese Academy of Sciences, (2011).
- [3] Xue Xiaoguang, Li Guoxi, Gong Jingzhong, et al. "Assembly process oriented computer aided alignment technology of precision optical system" *J. Computer Integrated Manufacturing Systems*, 17(10): 2163-2170 (2011).
- [4] JEONGH W, LAWRENCEGN, NAHM KB. "Auto-alignment of a three-mirror off-axis telescope by reverse optimization and end-to-end aberration measurements," *C. In Current Developments in Optical Engineering II, Proc. SPIE 818*, 419-430 (1987).
- [5] David M. Williamson. "Compensator selection in the tolerancing of a microlithographic lens," *J. Proceedings of SPIE*, 1049 (1989).
- [6] Tomoyuki Matsuyama, Issey Tanaka, et al. "Improving lens performance through the most recent lens manufacturing process," *J. Proceedings of SPIE*, 5040: 801-810 (2003).
- [7] Jan Mulkens, Jos de Klerk, et al. "Latest Developments on Immersion Exposure Systems," *J. Proceedings of SPIE*, 6924:69241P-1, 69241P-12 (2008).
- [8] Yasuhiro Ohmura, Taro Ogata, et al. "An aberration control of projection optics for multi-patterning lithography," *J. Proceedings of SPIE*, 7973:79730W-1, 79730W-11 (2011).
- [9] Katsumi Sugisaki, Tetsuya Oshjnoa, Katsuhiko Murakami, et al. "Assembly and alignment of three aspherical mirror optics for extreme ultraviolet projection lithography," *C. Proceedings of SPIE Vol.3997*: 751-758 (2000).
- [10] Tomoyuki Matsuyama, Yasuhiro Ohmura, Toshiharu Nakashima, et al. "An Intelligent Imaging System for ArF Scanner," *C. Proc. of SPIE Vol. 6924*: 69241S (2008).
- [11] Hirotaka Kohno, Yuichi Shibasaki, Jun Ishikawa, et al. "Latest performance of immersion scanner S620D with the Streamline platform for the double patterning generation," *C. Proceedings of SPIE Vol.7640*: 76401O (2010).
- [12] Zhang Tingcheng, Wang Yongtian, Chang Jun, et al. "Computer-aided alignment for reflective zoom systems," *J. Acta Optica Sinica*, 30(6): 1688-1692 (2010).
- [13] Kong Xiaohui, Fan Xuewu. "Alignment of two-mirror aspherical optical system based on vector aberration theory," *J. Laser & Optoelectronics Progress*, (8): 90-96 (2010).

Author Biographies



LU Yutong received M.Sc. degree from Changchun University of Science and Technology in 2011. She is currently an assistant engineer of the Institute of Optoelectronic Technology, Chinese Academy of Sciences Spacecraft Ground Calibration and Measurement. Her main research interest includes micro-nano optics.

E-mail: lytinkey@126.com



ZHOU Ji, Ph.D. degree. She is currently an assistant researcher. Her Main research interest includes micro-nano equipment structure.

E-mail: zhouji@whu.edu.cn

